THREE-BODY NUCLEAR REACTIONS FROM QUANTUM CHROMODYNAMICS

Nicholas C. Chambers* and Andrew W. Jackura (*advisor*)†
Department of Physics, William & Mary, Williamsburg, VA 23187, USA
(Dated: April 3, 2026)

Nuclear reactions are responsible for a broad collection of astrophysical phenomena. We review the state-of-the-art workflow for calculating properties of nuclear reactions from quantum chromodynamics (QCD), the relativistic quantum field theory governing the interactions of quarks and gluons. Decades of innovation in formal scattering theory and numerical methods such as lattice QCD have enabled precise, first-principles calculations of reactions involving *two particles*. However, nuclear reactions involving *three particles* are integral to the evolution of astrophysical systems like the Sun, neutron stars, and the early universe. We present an advancement in the construction of three-body scattering amplitudes, functions which describe the full details of three-body nuclear reactions. Additionally, we present a new approach in visualizing two-body subsystem dynamics within a full three-body reaction using an *intensity distribution* inspired by Dalitz plots, which are widely used by the nuclear physics community to study three-body decays of heavy particles.

I. INTRODUCTION

A longstanding goal within the nuclear physics community has been to bridge the gap between the unobservable quark and gluon degrees of freedom within quantum chromodynamics (QCD) to the observable properties of hadrons that comprise all ordinary matter in the universe. A subset of problems in this program are classified under *hadron spectroscopy*, the study of hadrons that form within multi-particle reactions governed by the strong nuclear force. Unlike the familiar proton and neutron, most hadrons are highly unstable *resonances* that are never directly observed in detectors within scattering experiments; instead, hadronic resonances must be *inferred* from enhancements (or "peaks") in scattering cross sections of stable hadrons. This contrasts hadron spectroscopy from the more familiar field of atomic spectroscopy, where excited states of atoms are determined through direct detection of photons emitted during relaxation to the ground state.

* e-mail: ncchambers@wm.edu
† e-mail: awjackura@wm.edu

Another complication in the hadron spectrum is that the states of interest, hadronic resonances, are embedded within the QCD scattering continuum. That is, resonances appear above multi-hadron thresholds, thereby requiring the use of scattering theory to describe the decay of these resonances to multi-hadron final states. In the case of resonances that appear in reactions of two hadrons, the scattering formalism is relatively simple. However, most resonances are heavy enough to decay into three (or more) particles, and therefore require a treatment of their dynamics within a *three-body* scattering formalism. Nuclear reactions are the starting point in key astrophysical processes, ranging from the evolution of matter in the Big Bang (BB) to nucleosynthesis in stars, so a predictive understanding of such reactions is essential to NASA's astrophysics goals.

Contemporary first-principles calculations of nuclear reactions rely on lattice QCD,[1] in which the dynamics of quarks and gluons are simulated numerically. Then, applying a non-perturbative technique known as the *Lüscher formalism*, the energy levels of the quark-gluon system in the finite volume are used to constrain

the corresponding infinite-volume *reaction amplitude* describing the scattering of observable hadrons. The analytic structure of these amplitudes yield predictions for observable features of nuclear reactions, such as reaction cross-sections and masses and lifetimes of resonances.[2]

Decades of innovation on this workflow have produced a wealth of results in two-body scattering of mesons and a growing number of results involving baryons.[1,3] However, many phenomena central to nuclear physics and astrophysics require a consistent treatment of *three-body* dynamics. For instance, it has been shown that even in the spectrum of light nuclei, three-body forces are responsible for a shift of up to twenty percent compared to analyses that use only two-body interactions.[4] Extending the successful lattice QCD workflow to accommodate three-body reactions was therefore the central objective of the broader project that resulted in this work.

Importantly, three-body nuclear interactions also arise in several systems that are relevant to NASA's science goals. For example, proton-deuteron (pd) scattering is a key input into the primordial deuterium-to-hydrogen (D/H) abundance ratio,[5–8] and accurate descriptions of the pd cross section require realistic three-nucleon ($3N$) interaction models.[9–12] As emphasized in Appendix C of the 2020 Decadal Survey of Astronomy and Astrophysics (Astro2020),[13] light element abundances serve as sensitive probes of possible dark-sector physics in the early universe — complementing constraints from missions such as NASA's WMAP[14] and the Hubble Space Telescope.[15] Three-body forces also play a central role in determining the neutron star equation of state (NS-EOS),[16–21] which describes the relationship between a star's mass and radius. Determining the NS-EOS is identified in Appendix B of Astro2020[13] as a key objective for NASA's astrophysics program. Because the NS-EOS is fundamentally determined by the underlying nuclear interactions in dense matter, advances in three-nucleon physics directly support this broader mission.

In the remainder of this work, we summarize contemporary methodology for computing reaction observables from lattice QCD, and we present our results on constructing partial wave (PW) projections of three-body scattering amplitudes. In Sec. II, we discuss the use of lattice QCD to compute correlation functions of quark/gluon field operators, whose data are used to construct a scattering amplitude. By analytically continuing the amplitude to complex energy, one extracts properties of hadronic resonances from a corresponding pole location. In Sec. III, we discuss the main results of this work, a technical procedure known as *symmetrization*, which is necessary to construct three-body PW amplitudes.

II. HADRON SPECTROSCOPY FROM QCD

At the energy scales relevant for hadron physics, calculations within QCD are necessarily *nonperturbative* and therefore must be completed numerically. The current state-of-the-art numerical method for QCD calculations is lattice QCD, which simulates the time-dependence of correlation functions of quark-gluon field operators within a finite, discretized spacetime lattice. Using operators $\mathcal{O}^{\mathfrak{q}}(t)$, where $\mathfrak{q}$ is a generalized index corresponding to the quantum numbers of our system (including parity, spin, isospin, etc.), we construct two-point correlation functions of the form

$$C(\tau) \equiv \langle 0|\mathcal{O}^{\mathfrak{q}}(\tau)(\mathcal{O}^{\mathfrak{q}}(0))^{\dagger}|0\rangle. \qquad (1)$$

Then, we access the eigenstates of QCD in the finite volume through a spectral decomposition given by

$$C(\tau) = \sum_{\mathfrak{n}} Z_{\mathfrak{n}} Z_{\mathfrak{n}}^{\dagger} e^{-E_{\mathfrak{n}}\tau}, \qquad (2)$$

where $Z_{\mathfrak{n}}$ is the overlap matrix element of $\mathcal{O}^{\mathfrak{q}}$ onto the finite-volume energy eigenstate $|\mathfrak{n}\rangle$ and $E_{\mathfrak{n}}$ is the corresponding en-

ergy eigenvalue. Using a collection of many operators $\{\mathcal{O}_i^{\mathfrak{q}}\}_{i=1}^N$, we obtain a discrete set of energy levels $\{E_{\mathfrak{n}}\}$ which correspond to the spectrum of QCD confined to the finite-volume lattice — analogous to the discrete spectrum obtained from the traditional "particle-in-a-box" problem from non-relativistic quantum mechanics.

Of course, one must connect this finite-volume data, which depends on the QCD interaction, to nuclear reactions in the infinite-volume. This mapping is captured through a collection of results within the so-called *Lüscher formalism*.[1,2] Omitting detail, the finite-volume spectra $\{E_{\mathfrak{n}}\}$ define the points at which a *Lüscher quantization* is satisfied:

$$\det\left(F^{-1}(E_{\mathfrak{n}}, L) + \mathcal{K}_2(E_{\mathfrak{n}})\right) = 0. \qquad (3)$$

Here, F is a finite-volume kinematic function that depends on, among other things, the finite size of the lattice L, whereas $\mathcal{K}_2$ is referred to as a "K-matrix" and encodes the QCD interaction between scattered particles in the infinite volume. One can think of the K-matrix as generalizing the scattering phase shift $\delta(E)$ from ordinary, non-relativistic scattering theory — a generalization which has use in three-body scattering, where the notion of a "phase-shift" is less clear. Both functions are taken as matrices in (ℓ, m)-space, where ℓ is the angular momentum of the system and m is its projection onto some axis*. For each energy level extracted from the lattice, we solve Eq. (3) for a value of the K-matrix, then fit these values to some parameterization of $\mathcal{K}_2(E)$. For instance, we might try the effective range expansion for elastic scattering near threshold,

$$\mathcal{K}_2^{-1}(E) = -\frac{1}{a} + \frac{1}{2}r(E^2/4 - m^2) + \mathcal{O}(E^3). \qquad (4)$$

Then, by fitting parameters a and r to the outputs of the Lüscher quantization condition, we may reconstruct an analytic representation for the reaction amplitude,

$$\mathcal{M}_2^J(E) = \frac{1}{\mathcal{K}_2^J(E)^{-1} - i\rho(E)}, \qquad (5)$$

where $\rho(E) \propto \sqrt{1 - 4m^2/E}$. Notice in Eq. (5) that, instead of the full $\mathbf{2} \to \mathbf{2}$ reaction amplitude, which depends on E and the scattering angle θ, we have constructed a *PW projection* of $\mathcal{M}_2$ to definite angular momentum J. By working with PW projections, we simplify the kinematics of our amplitude, and we have direct knowledge that any resonances which appear in $\mathcal{M}_2^J$ will be of spin J. For example, if one wishes to study the well-known, spin-1 $\rho(770)$ resonance in $\pi\pi$ scattering, one would identify it as a pole in the $J = 1$ PW projection of $\mathcal{M}_2$.

With an analytic representation of $\mathcal{M}_2^J$, like in Eq. (5), one now has, in principle, full knowledge of the reaction within the PW channel J. From here, one can extract observable quantities from the amplitude and compare them with experimental results. For example, one can construct the scattering cross section by summing the mod-squared PW amplitudes, $\sigma(E) \propto \sum_J |\mathcal{M}_2^J(E)|^2$. Other observable information, relevant to the hadron spectroscopy community, are resonance properties within these reaction amplitudes. These are found via *analytic continuation* of the PW amplitude to complex energy and, if a resonance is present in this definite-J channel, determining a pole location. The location of the pole is related to the mass M and decay width Γ of the resonance via

$$E_{\text{pole}} = M - i\frac{\Gamma}{2}. \qquad (6)$$

Organizations such as the Hadron Spectrum Collaboration (Hadspec) have produced many results for hadronic reaction amplitudes, including resonant and nonresonant elastic scattering, and

* Since the continuous rotational symmetry of the infinite-volume system is broken on the cubic lattice, F will not be a diagonal matrix in (ℓ, m)-space.

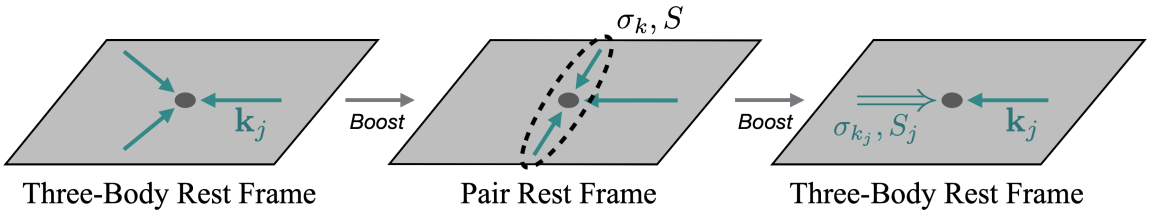

FIG. 1. Kinematics of the PW projection of a three-body system in the pair-spectator basis.

coupled-channel processes.[22] Experiments like GlueX at Jefferson Lab have the primary objective of collecting data on low-lying hadronic resonances, including the so-called "exotic" resonances that defy traditional quark model expectations. Hadspec has complemented this effort with precision calculations of $\pi\pi$ scattering[23–25] and pion photoproduction[26] amplitudes used to extract properties of benchmark resonances like the ρ and b_1[27] as well as elusive resonances like the π_1.[28] In fact, the theoretical exploration of Hadspec has been instrumental in proposing new directions to search for the π_1 in GlueX, such as in $\pi_1 \to b_1\pi \to \omega\pi\pi$.[29]

Three-body calculations on the lattice are in their infancy, with the earliest taking place only a few years ago.[30–32] The workflow for computing observables of three-body reactions from QCD remains largely the same as in the two-body case. The operators $\mathcal{O}^{\mathfrak{q}}$ which are simulated on the lattice are now divided into (i) operators $\mathcal{O}_2^{\mathfrak{q}_2}$ which overlap onto the two-body subchannels $\mathfrak{q}_2$ that contribute to the three-body process and (ii) operators $\mathcal{O}_3^{\mathfrak{q}}$ which overlap onto the total three-body target quantum numbers $\mathfrak{q}$. These operators contribute to their respective correlation functions, Eq. (1), which are used to extract two- and three-body finite-volume spectra. These spectra are then used as inputs into two- and three-body Lüscher quantization conditions, analogous to Eq. (3), which are used to fit two- and three-body K-matrix parameters. Similar to Eq. (5), there are known representations of the three-body PW projected amplitude $\mathcal{M}_3$, which take the form of coupled integral equations,[33] in terms of two- and three-body K-matrices $\mathcal{K}_2$ and $\mathcal{K}_3$. The following section, and the main body of results in this work, concerns a set of technical details that arise in constructing analytic expressions for three-body PW amplitudes.

III. SYMMETRIZATION OF PARTIAL WAVE AMPLITUDES

There are several methods for constructing PW projections of three-body amplitudes, but one that is used commonly across the relevant literature is the so-called "pair-spectator" basis. This approach leverages the familiar two-body scattering formalism by performing a sequence of two two-body PW projections. In the three-body rest frame, one particle is designated the role of 'spectator' while the remaining two form an interacting pair. The two momenta of the pair are PW projected in the pair rest frame, followed by a PW projection between the pair subsystem and the spectator in the three-body rest frame (see Fig. 1). Although this PW basis is a natural approach with familiar kinematics, its weaknesses become apparent during the process of *symmetrization*. Because the pair-spectator basis begins with singling out one of the three momenta in the system, we introduce an unphysical dependence of our PW amplitude on the spectator's kinematics and denote the resulting PW amplitude $\mathcal{M}_3^{J\,(j',j)}$, where $j', j \in \{1, 2, 3\}$ denote which of the momenta correspond to the incoming and outgoing spectators. Thus, we symmetrize the PW amplitude by summing over this choice of spectator in the incoming and

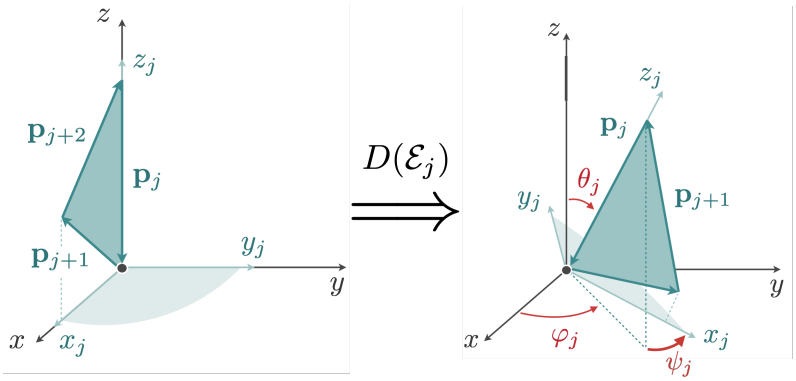

FIG. 2. Euler angles $\mathcal{E}_j = (\phi_j, \theta_j, \psi_j)$ that define the orientation of the three-body rest frame with respect to a space-fixed coordinate system associated with spectator j.

outgoing state,

$$\mathcal{M}_3 = \sum_{j'j} \mathcal{M}_3^{(j',j)}. \tag{7}$$

Note that throughout the rest of this work, I will use primed variables to represent outgoing kinematics, while unprimed variables represent kinematics in the incident state. I will refer to 'spectator j' as well as the pair associated with spectator j as 'pair j' (see Fig. 1). Simplifying Eq. (7) within the pair-spectator basis is quite challenging, as there comes a step in which one must integrate the angular kinematics in the rest frame of pair j with respect to the angular kinematics associated to a *different* pair rest frame, e.g. pair $j+1$. Further details can be found in Appendix A of the article associated with this report.[34] We presented in that article a procedure for simplifying Eq. (7) using a different PW basis, which I will subsequently refer to as the "Dalitz" basis*. In the Dalitz basis, all the angular kinematics of the three-body amplitude are isolated in the three-body rest frame, thereby avoiding the complicated angular integrations across multiple Lorentz frames needed for the symmetrization procedure within the pair-spectator basis. To PW project the three-body amplitude within the Dalitz basis, we define a *body-fixed* coordinate system $(x_j y_j z_j)$ that is fixed to the *reaction plane* (the rigid body formed by the incident/outgoing momenta in the three-body rest frame) in the initial/final state and oriented such that the z_j axis is anti-aligned with the momentum of spectator j. We then define an orientation of this reaction plane with respect to a *space-fixed* coordinate system (XYZ) using Euler angles $\mathcal{E}_j = (\phi_j, \theta_j, \psi_j)$ (see Fig. 2), and we obtain a PW projection of the three-body amplitude in the form

$$\begin{aligned}\mathcal{M}^{(j',j)}(\{\mathbf{p}'\},\{\mathbf{p}\}) = \\ \sum_{J,m_J}\sum_{\lambda'_{j'},\lambda_j} (2J+1)\, D^{(J)*}_{m_J\lambda'_{j'}}(\mathcal{E}'_{j'}) \\ \times \mathcal{M}^{J\,(j',j)}_{\lambda'_{j'}\lambda_j}(\{\sigma'\},\{\sigma\})\, D^{(J)}_{m_J\lambda_j}(\mathcal{E}_j).\end{aligned} \tag{8}$$

Here, $\mathcal{M}^{J\,(j',j)}_{\lambda'_{j'},\lambda_j}$ is the *unsymmetrized* "Dalitz" PW amplitude of definite angular momentum J; $\lambda'_{j'}$ and λ_j represent the outgoing and incoming helicities of the three-particle system along the body-fixed $z'_{j'}$ and z_j axes, respectively; $\{\sigma'\} = \{\sigma'_1, \sigma'_2, \sigma'_3\}$ and $\{\sigma\} = \{\sigma_1, \sigma_2, \sigma_3\}$ represent the Lorentz invariant masses of the two-particle pair subsystems associated to each spectator, $\sigma_j = (p_{j+1} + p_{j+2})^2$; and the D functions are Wigner-D matrix elements.

Now, the process of symmetrizing the Dalitz PW amplitudes of Eq. (8) is much

* N.B. this basis is not our invention and is a standard basis for the PW projection of any quantum state sharing the rotational properties of a rigid body. See Sec. 7.5d in Gottfried and Yan.[35]

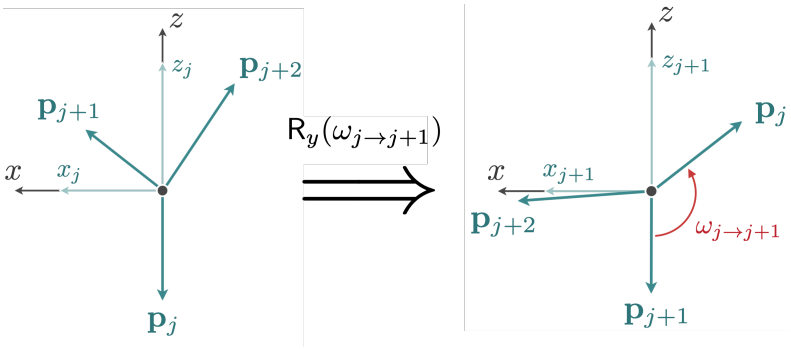

FIG. 3. Changing to a different choice of spectator amounts to a rotation about the Y axis of the three-body rest frame.

more tractable than the PW amplitudes of the pair-spectator basis. To change the choice of spectator from e.g., spectator j to spectator $j+1$ in the PW procedure in the Dalitz basis, one simply rotates the reaction plane (thereby rotating the body-fixed coordinate system) such that spectator momentum $\mathbf{p}_{j+1}$ is anti-aligned with the space-fixed Z axis. Since the Dalitz PW projection is performed entirely in the three-body rest frame, this amounts to a simple rotation about the space-fixed Y axis (see Fig. 3). This is represented on the level of state vectors in the Dalitz PW basis as

$$|\{\sigma\}, Jm_J, \lambda_{j+1}\rangle = \sum_{\lambda'_j} \left|\{\sigma\}, Jm_J, \lambda'_j\right\rangle d^{(J)}_{\lambda_a\lambda'_j}(\omega_{j\to j+1}), \quad (9)$$

where d is the Wigner little-d matrix element, and $\omega_{j\to j+1}$ is the signed angle between spectator momenta $\mathbf{p}_j$ and $\mathbf{p}_{j+1}$ in the three-body rest frame.

Having defined the rotational scheme for symmetrization, summarized by Eq. (9), we may start simplifying Eq. (7) in the Dalitz basis by inverting Eq. (8),

$$\mathcal{M}^{J\,(j',j)}_{\lambda'_{j'}\lambda_j}(\{\sigma'\},\{\sigma\}) = \frac{1}{(8\pi^2)^2}\sum_{m_J}\int \mathrm{d}\mathcal{E}'_{j'}\int \mathrm{d}\mathcal{E}_j D^{(J)}_{m_J\lambda'_{j'}}(\mathcal{E}'_{j'})\,\mathcal{M}^{(j',j)}(\{\mathbf{p}'\},\{\mathbf{p}\})\,D^{(J)*}_{m_J\lambda_j}(\mathcal{E}_j). \quad (10)$$

with the integration measure defined as $\mathrm{d}\mathcal{E} = \mathrm{d}\phi\mathrm{d}\cos\theta\mathrm{d}\psi$ over the domain $\phi,\psi \in [0,2\pi)$ and $\theta \in [0,\pi)$. Then, instead of the unsymmetrized amplitude $\mathcal{M}^{(j',j)}(\{\mathbf{p}'\},\{\mathbf{p}\})$, we insert the symmetrized amplitude $\mathcal{M}(\{\mathbf{p}'\},\{\mathbf{p}\})$ in the RHS of Eq. (10) and then apply Eq. (7) to obtain

$$
\begin{aligned}
&\mathcal{M}^{J}_{\lambda'_{a'}\lambda_a}(\{\sigma'\},\{\sigma\}) = \\
&\quad \frac{1}{(8\pi^2)^2}\sum_{m_J}\sum_{j',j}\int \mathrm{d}\mathcal{E}'_{a'}\int \mathrm{d}\mathcal{E}_a D^{(J)}_{m_J\lambda'_{a'}}(\mathcal{E}'_{a'})\,\mathcal{M}^{(j',j)}(\{\mathbf{p}'\},\{\mathbf{p}\})\,D^{(J)*}_{m_J\lambda_a}(\mathcal{E}_a) \\
&\quad = \frac{2J+1}{(8\pi^2)^2}\sum_{m_J}\sum_{j',j}\sum_{J'm'_{j'}}\sum_{\mu'_{j'}\mu_j}\int \mathrm{d}\mathcal{E}'_{a'} D^{(J)}_{m_J\lambda'_{a'}}(\mathcal{E}'_{a'})\,D^{(J')*}_{m'_{J'}\mu'_{j'}}(\mathcal{E}'_{j'}) \\
&\qquad \times \mathcal{M}^{J\,(j',j)}(\{\sigma'\},\{\sigma\})\int \mathrm{d}\mathcal{E}_a\, D^{(J)*}_{m_J\lambda_a}(\mathcal{E}_a)\,D^{(J)}_{m'_{j'}\mu_j}(\mathcal{E}_j)
\end{aligned}
\tag{11}
$$

where, in going from the second to third line of Eq. (11), we have re-expressed the unsymmetrized amplitude $\mathcal{M}^{(j',j)}(\{\mathbf{p}'\},\{\mathbf{p}\})$ in the Dalitz PW basis (Eq. (8)). Notice we have distinguished the spectator labels associated with the symmetrized amplitude (a' and a) from those of the unsymmetrized amplitude (j' and j). To simplify Eq. (11), we use the addition property of the Wigner-D matrices to write

$$
D^{(J)}_{m_J\lambda'_j}(\mathcal{E}_j) = \sum_{\mu} D^{(J)}_{m_J\mu}(\mathcal{E}_a)\,d^{(J)}_{\mu\lambda'_j}(\omega_{j\to a}).
\tag{12}
$$

Then, using the orthogonality of the Wigner-D matrices over the $\mathrm{d}\mathcal{E}$-integration measure, we obtain a simplified and computable form for the symmetrized Dalitz PW amplitude,

$$
\begin{aligned}
&\mathcal{M}^{J}_{\lambda'_{a'}\lambda_a}(\{\sigma'\},\{\sigma\}) = \\
&\quad \sum_{j'j}\sum_{\mu'_{j'},\mu_j} d^{(J)}_{\lambda'_{a'}\mu'_{j'}}(\omega'_{j'\to a'}) \\
&\qquad \times \mathcal{M}^{J\,(j',j)}_{\mu'_{j'}\mu_j}(\{\sigma'\},\{\sigma\})\,d^{(J)}_{\lambda_a\mu_j}(\omega_{j\to a}).
\end{aligned}
\tag{13}
$$

Having obtained a useful form for the symmetrized PW amplitude in the Dalitz basis, Eq. (13), we now wish to connect back to the pair-spectator basis, in which many prior results for three-body PW projection are established. We use the change of basis given in our symmetrization article[34] (Eq. 35 of that work) to write $\mathcal{M}^{J\,(j',j)}_{\mu'_{j'}\mu_j}(\{\sigma'\},\{\sigma\})$ in Eq. (13) in terms of the spin-orbit pair-spectator amplitude, yielding the main result of our previous work,[34]

$$
\begin{aligned}
&\mathcal{M}^{J^P}_{\lambda'_{a'}\lambda_a}(\{\sigma'\},\{\sigma\}) = \\
&\quad \sum_{j'j}\sum_{L'_{j'}S'_{j'}}\sum_{L_jS_j}\left(\mathcal{R}^{J^P}_{j'\to a'}\right)_{L'_{j'}S'_{j'};\lambda'_{a'}} \\
&\qquad \times \mathcal{M}^{J^P\,(j',j)}_{L'_{j'}S'_{j'};L_jS_j}(p',p)\left(\mathcal{R}^{J^P}_{j\to a}\right)_{L_jS_j;\lambda_a},
\end{aligned}
\tag{14}
$$

where $\mathcal{R}$ is a *recoupling coefficient* defined as

$$
\begin{aligned}
\left(\mathcal{R}^{J^P}_{j\to a}\right)_{L_jS_j;\lambda_a} &\equiv \sum_{\mu_j} d^{(J)}_{\lambda_a\mu_j}(\omega_{j\to a}) \\
&\quad \times d^{(S_j)}_{\mu_j 0}(\theta^\star_j)\mathcal{P}_{\mu_j}(J,L_j,S_j).
\end{aligned}
\tag{15}
$$

where S is the total angular momentum of the pair subsystem, L is the relative angular momentum between the pair and spectator, $\theta^\star_j$ is the polar angle of the pair subsystem in its rest frame, and $\mathcal{P}$ is proportional to a Clebsch-Gordan coefficient connecting L, S and J. An additional detail not included in this report is the symmetrization of the SU(2) isospin coupling procedure for the three-particle system. See Sec. 3b of our symmetrization article for further details.

Now that the unphysical spectator dependence has been removed from our PW amplitude, we can construct something resembling a physically observable *intensity*

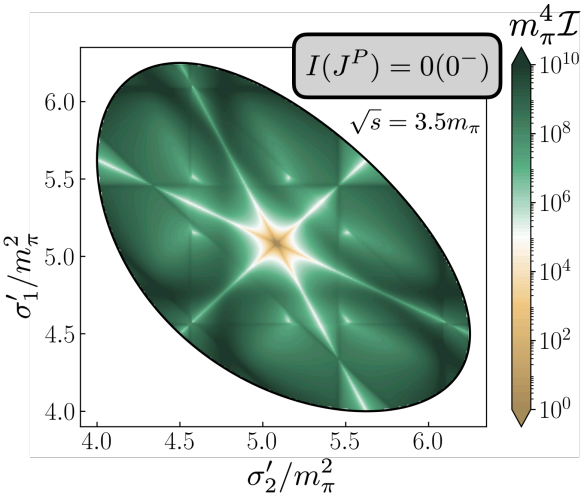

FIG. 4. Dalitz PW intensity distribution, Eq. (16), for $I(J^P) = 0(0^-)$ at fixed energy $\sqrt{s} = 3.5m_\pi$.

distribution.[*] We define a PW intensity distribution as the following:

$$\mathcal{I}^{I(J^P)}(\{\sigma'\},\{\sigma\}) \equiv \sum_{I'_{a'},I_a} \sum_{\lambda'_{a'}\lambda_a} \left|\mathcal{M}^{J^P}_{\lambda'_{a'}\lambda_a}(\{\sigma'\},\{\sigma\})\right|^2. \quad (16)$$

Note we have introduced the label I to represent the total three-body isospin, while I_a and $I'_{a'}$ represent the isospins of the two-body pair subsystems associated with spectators a and a'. $\mathcal{I}^{I(J^P)}$ is a function of five independent degrees of freedom: total energy $\sqrt{s}$, two σ-variables for the initial state, and two σ'-variables for the final state. If I fix the initial kinematics of my system, then $\mathcal{I}^{I(J^P)}$ will be a distribution in two final state pair invariant masses $\sigma'_{a'}$, and $\sigma'_{a'+1}$ — which are the same kinematics of a *Dalitz distribution* used widely in the hadron physics community to visualize the three-body decays of heavy particles. A useful check on our final result for the symmetrized three-body PW amplitude, Eq. (14), is to compare the symmetry features of the Dalitz distributions we construct to those previously predicted using known symmetries of 3π decays.[37]

We therefore apply our symmetrized PW amplitude to a model of 3π elastic scattering. On-shell representations of the pair-spectator amplitude $\mathcal{M}^{J^P\,(j',j)}_{L'_{j'}S'_{j'}I'_{j'};\,L_jS_jI_j}(p',p)$ are constructed as a set of coupled integral equations,[33] but, under the assumption that the full three-body interaction can be described by a sequence of pairwise exchanges between two-body interactions (see Sec. V in our prior work[34] for details), we may approximate the solution to these integral equations as the following,

$$\mathcal{M}^{J^P\,(j',j)}_{L'_{j'}S'_{j'}I'_{j'};\,L_jS_jI_j}(p',p) = -\mathcal{M}^{I'_{j'}}_{2;\,S'_{j'}}(\sigma'_{j'}) \times \mathcal{G}^{J^P}_{L'_{j'}S'_{j'}I'_{j'};\,L_jS_jI_j}(p',p)\,\mathcal{M}^{I_j}_{2;\,S_j}(\sigma_j). \quad (17)$$

where $\mathcal{M}^{I_2}_{2;\,S}$ is the two-body PW scattering amplitude of definite two-body isospin I_2 and angular momentum S, and $\mathcal{G}^{J^P}$ is the PW one-particle exchange (OPE) propagator that characterizes the exchange of a spectator particle between incoming and outgoing pairs. Details of the OPE function, including its PW projection, can be found in prior works by Jackura, Briceño, and Costa.[38,39]

At this point, dynamical information is needed as an input for the two-body interactions, $\mathcal{M}_2$ in Eq. (17), and we use $\pi\pi$ scattering phase shift data that was previously computed by Hadspec in prior lattice QCD analyses (see Sec. V of our symmetrization article).[34] Our input data includes S-wave phase shifts for $I_2 = 0$ and $I_2 = 2$ $\pi\pi$ scattering, parameterized by an effective range expansion, and a P-wave $I_2 = 1$ phase shift parameterized by a Breit-Wigner model. This Breit-Wigner phase shift characterizes the narrow ρ resonance which, at this heavier-than-physical pion mass, is centered at $m_\rho \approx 2.15m_\pi$.

[*] It would not be fair to describe the following distribution functions as observable — as they contain kinematic singularities which would not be measured in a $\mathbf{3} \to \mathbf{3}$ scattering process. Constructing physically realizable observables, such as a cross section, is nontrivial for $\mathbf{3} \to \mathbf{3}$ reactions. See Potapov and Taylor for further details.[36]

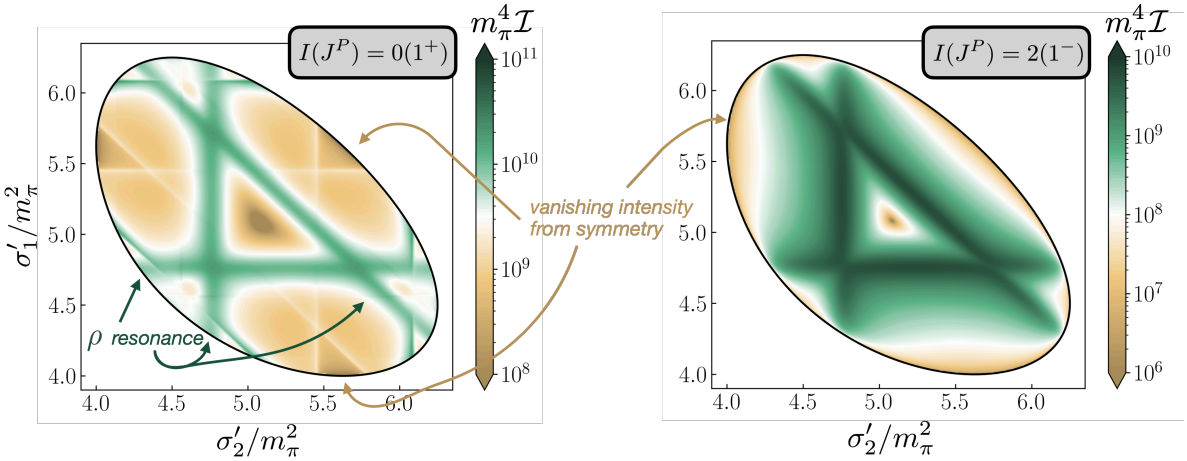

FIG. 5. Same distribution as in Fig. 4, but for $I(J^P) = 0(1^+)$ (left) and $I(J^P) = 2(1^-)$.

We now showcase a set of Dalitz distributions for a few choices of three-body PW quantum numbers $I(J^P)$. We start with $I(J^P) = 0(0^-)$ (Fig. 4), and we immediately see a striking sixfold symmetry in the body of the plot. Because the 3π system is constrained by generalized Bose symmetry, there will be symmetry structures in the Dalitz distribution where the intensity vanishes. We have three *nodal lines* corresponding to any two of the σ'-variables being equal. In the center of the plot, where the nodal lines overlap, we have an even more rapid vanishing of the distribution. Notably, we have close agreement with prior predictions by Zemach in this channel.[37] Our symmetrized PW amplitude can also be constructed for higher angular momenta $J = 1$, yielding the Dalitz plots of Fig. 5. Distinct features of these distributions include enhancements due to the ρ resonance in the $\pi\pi$ subsystems, visualized by the bands around $\sigma' \approx 4.6m_\pi^2$. Since our amplitude is symmetrized, we see reflections of the resonant bands and symmetry nodes in the other σ' variables of the Dalitz plot.

IV. SUMMARY

We have reviewed contemporary methodology for predicting properties of nuclear/hadronic reactions from first-principles QCD. The frontier of these tools is being extended into calculations of $\mathbf{3} \to \mathbf{3}$ reactions, which are ubiquitous across nuclear physics and astrophysics. We have presented a solution to a problem in three-body scattering amplitude analysis, providing a construction of PW amplitudes that have a closer connection to physical observables studied in experiments. We gave a sketch of the derivation presented in our prior work,[34] which symmetrizes PW projections of the three-body amplitude. This allowed us to construct intensity distributions which closely resemble the widely-used Dalitz plots. We implemented a model of 3π scattering in our symmetrized amplitude, and demonstrated that our intensity distributions exhibited the symmetry features one would expect of three-pion decays. Among these features were enhancements from the ρ resonance in each $\pi\pi$ subsystem and locations where the distribution vanished due to the Bose symmetry of the 3π system. The symmetrization procedure is the final step of the broader workflow of computing reaction observables from lattice QCD, and our results have already been applied in subsequent 3π lattice studies.[40] Looking forward, further generalization of our construction is still needed, including extensions to particles with intrinsic spin and to systems with coupled two- and three-body scattering channels.

[1] R. A. Briceno, J. J. Dudek, and R. D. Young, Rev. Mod. Phys. **90**, 025001 (2018).

[2] M. Albaladejo *et al.* (JPAC), (2021), 10.1016/j.ppnp.2022.103981.

[3] B. Hörz *et al.*, Phys. Rev. C **103**, 014003 (2021).

[4] M. Piarulli *et al.*, Phys. Rev. Lett. **120**, 052503 (2018).

[5] T.-H. Yeh *et al.*, JCAP **03**, 046 (2021).

[6] C. Pitrou, A. Coc, *et al.*, Monthly Notices of the Royal Astronomical Society **502**, 2474 (2021).

[7] O. Pisanti *et al.*, JCAP **04**, 020 (2021).

[8] V. Mossa, K. Stöckel, F. Cavanna, *et al.*, Nature **587**, 210 (2020).

[9] L. E. Marcucci, G. Mangano, A. Kievsky, and M. Viviani, Phys. Rev. Lett. **116**, 102501 (2016).

[10] K. Ermisch *et al.*, Phys. Rev. C **71**, 064004 (2005).

[11] A. Ramazani-Moghaddam-Arani *et al.*, Phys. Rev. C **78**, 014006 (2008).

[12] A. Deltuva, Phys. Rev. C **80**, 064002 (2009).

[13] National Academies of Sciences, Engineering, and Medicine, *Pathways to Discovery in Astronomy and Astrophysics for the 2020s* (The National Academies Press, 2023).

[14] J. Dunkley *et al.*, ApJS **180** (2009).

[15] N. H. M. Crighton, J. K. Webb, *et al.*, Monthly Notices of the Royal Astronomical Society **345**, 243 (2003).

[16] A. W. Steiner and S. Gandolfi, Phys. Rev. Lett. **108**, 081102 (2012).

[17] S. Gandolfi, A. Y. Illarionov, *et al.*, Monthly Notices of the Royal Astronomical Society: Letters **404**, 35 (2010).

[18] S. Gandolfi *et al.*, Phys. Rev. C **79**, 054005 (2009).

[19] S. Gandolfi, J. Carlson, and S. Reddy, Phys. Rev. C **85**, 032801 (2012).

[20] X. R. Zhou *et al.*, Phys. Rev. C **69**, 018801 (2004).

[21] Z. H. Li and H.-J. Schulze, Phys. Rev. C **78**, 028801 (2008).

[22] J. J. Dudek, R. G. Edwards, and D. J. Wilson, Phys. Rev. D **93**, 094506 (2016).

[23] J. J. Dudek, R. G. Edwards, *et al.*, Phys. Rev. **D83**, 071504 (2011).

[24] J. J. Dudek, R. G. Edwards, and C. E. Thomas, Phys. Rev. **D86**, 034031 (2012).

[25] J. J. Dudek, R. G. Edwards, and C. E. Thomas (Hadron Spectrum), Phys. Rev. **D87**, 034505 (2013).

[26] R. A. Briceño, J. J. Dudek, R. G. Edwards, *et al.*, Phys. Rev. **D93**, 114508 (2016).

[27] A. J. Woss, C. E. Thomas, J. J. Dudek, R. G. Edwards, and D. J. Wilson, Phys. Rev. D **100**, 054506 (2019).

[28] A. J. Woss, J. J. Dudek, Edwards, *et al.*, Phys. Rev. D **103**, 054502 (2021).

[29] F. Afzal *et al.* (The GlueX Collaboration), Phys. Rev. Lett. **133**, 261903 (2024).

[30] M. T. Hansen, R. A. Briceño, R. G. Edwards, *et al.* (Hadron Spectrum), Phys. Rev. Lett. **126**, 012001 (2021).

[31] B. Hörz and A. Hanlon, Phys. Rev. Lett. **123**, 142002 (2019).

[32] C. Culver, M. Mai, R. Brett, A. Alexandru, and M. Döring, Phys. Rev. D **101**, 114507 (2020).

[33] A. W. Jackura, Phys. Rev. D **108**, 034505 (2023).

[34] A. W. Jackura, **N. C. Chambers**, and R. A. Briceño, Phys. Rev. D **113**, 014019 (2026).

[35] K. Gottfried and T.-M. Yan, *Quantum Mechanics: Fundamentals* (Springer-Verlag New York, Inc., 2003).

[36] V. S. Potapov and J. R. Taylor, Phys. Rev. A **16**, 2264 (1977).

[37] C. Zemach, Phys. Rev. **133**, B1201 (1964).

[38] A. W. Jackura and R. A. Briceño, Phys. Rev. D **109**, 096030 (2024).

[39] R. A. Briceño, C. S. R. Costa, and A. W. Jackura, Phys. Rev. D **111**, 036029 (2025).

[40] R. A. Briceño, M. T. Hansen, *et al.*, (2025), arXiv:2510.24894 [hep-lat].